Hamiltonian mapping of magnetic reconnection during the crash stage of the sawtooth instability

I. Pavlenko[a]
Université Libre de Bruxelles, Association EURATOM-Etat Belge, CP 231, Campus Plaine, 1050 Bruxelles, Belgium

B. Rapoport
Harvard University, 372 Lowell Mail Center, Cambridge, Massachusetts 02138

B. Weyssow and D. Carati
Université Libre de Bruxelles, Association EURATOM-Etat Belge, CP 231, Campus Plaine, 1050 Bruxelles, Belgium

(Received 1 November 2002; accepted 22 January 2003)

Since the determination of the magnetic field topology and of the safety factor profile during the crash stage of the sawtooth instability is a difficult problem both theoretically and experimentally, a complementary approach based on a mapping technique usually referred to as the Tokamap [Balescu *et al.*, Phys. Rev. E **58**, 951 (1998)] is proposed to reconstruct the stochastic magnetic field evolution. It is shown that this method, when combined with the constraints on the magnetic fluxes provided by the theories of the sawtooth instability, is able to generate poloidal cross sections of the magnetic field topology during the crash phase of the instability that have behavior similar to the experimental ones. The method is applied to both the complete and the incomplete reconnection of the magnetic field. © *2003 American Institute of Physics.* [DOI: 10.1063/1.1561279]

I. INTRODUCTION

Sawtooth oscillations of the plasma parameters in the central region of a tokamak plasma are observed when the safety factor, $q(r)$, falls below unity on the magnetic axis. These oscillations have a slow stage during which the plasma temperature and density rise, and a fast stage during which these parameters "crash." The central safety factor profile becomes flatter during the crash stage, although it undergoes only small relative changes. Nevertheless, the sensitive dependence of the magnetic field topology on the q-profile, and in particular on the magnetic shear, $d\log(q)/d\log(r)$, is an important factor in determining the magnetic field stochasticity, which in turn influences the turbulent transport. After the crash the experimentally observed temperature and density profiles flatten near the plasma center just due to the increased transport.

Experimental determination of the q-profile during the crash stage is problematic. The standard techniques used for experimental q-profile determination are Faraday rotation,[1] the motion stark effect (MSE)[2–4] and the toroidicity and ellipticity induced Alfvén eigenmode (TAE and EAE)[5–7] measurements. But Faraday rotation and MSE cannot resolve q fluctuations on time scales shorter than several milliseconds,[1,2] and measurement of the q-profile by TAE and EAE is limited by the resolution time of the Thomson scattering system, which is 100 ms.[5] By contrast, the crash stage of the sawtooth instability is typically on the order of 100 μs. Moreover, the central q value, $q_0 \equiv q(r=0)$, is particularly difficult to extract with precision from both MSE and TAE data,[6] and the experimental error of such measurements is typically around 10%.[7] This error value is sufficiently large to allow for some freedom in reconstructing the q-profile evolution in the center during the crash stage. In the same time the TAE and EAE allow us to get information on the q-profile before and immediately after sawtooth crashes with good accuracy.[5]

Several models have been proposed to explain the sawtooth instability (see, for example, Refs. 8–13). All these models differ with respect to q_0 after the crash and/or in the detailed behavior of the q-profile. To give two examples of different q-profile evolution with $q_0 < 1$, (a) the stochastic magnetic field model of the sawtooth instability[12] predicts an important role of the magnetic field stochasticity in the case of the partial magnetic reconnection even with the monotonic q-profile, and (b) the incomplete model of the reconnection based on the Taylor relaxation process[13] predicts the low magnetic shear in the center and around $q=1$. In fact the two models are not independent since the magnetic field stochasticity depends strongly on the magnetic shear value. Both of the models provide an increased turbulent transport in the plasma core causing the observed crash of the plasma parameters.

In the present work we apply a Hamiltonian mapping technique to model the magnetic field topology during the crash stage of the sawtooth instability. Our modeling is based on constraints imposed by the main theoretical models, and we compare our results with other descriptions of nonlinear behavior of the resistive mode. The remainder of this article is structured as follows. A short description of the Tokamap is given in Sec. II. Section III summarizes the key features of

[a]Permanent address: Kharkiv National University, Svobody sq.4, 61077 Kharkiv, Ukraine; electronic mail: ypavlenk@ulb.ac.be

the main theoretical models of reconnection. We present the results of our magnetic field modeling in Sec. IV. Section V discusses the relationships among our results, current theoretical models and experimental data. Finally, a summary and the conclusions are presented in Sec. VI.

II. THE TOKAMAP: A HAMILTONIAN MAPPING DESCRIPTION OF THE TOKAMAK MAGNETIC FIELD TOPOLOGY

The Tokamap has been proposed as a simple procedure for describing the magnetic field topology in toroidal magnetic confinement devices.[14] This technique does not exactly solve the magnetic field equations, but uses an approximation that reproduces the main features of the stochastic magnetic field. The Tokamap describes a poloidal cross-section of the field, (ψ,θ), where the dimensionless magnetic flux through a surface perpendicular to the magnetic axis, ψ (toroidal flux), has been chosen as a radial coordinate and θ is the poloidal angle. In the case of the circular torus ψ is related to the dimensionless radial coordinate, r (normalized to the plasma radius), by $\psi=r^2$ and in the unperturbed field the magnetic surfaces appear in cross-section as perfect nested circles.

If ζ is the toroidal angle and $\alpha_0(\psi)$ is the dimensionless poloidal flux, then the magnetic field line equations can be written in the following Hamiltonian form:

$$\frac{d\psi}{d\zeta}=-\frac{\partial\alpha_0}{\partial\theta}, \tag{1}$$

$$\frac{d\theta}{d\zeta}=\frac{\partial\alpha_0}{\partial\psi}, \tag{2}$$

where α_0 plays the role of the Hamiltonian. In the case of a perturbed magnetic field the perturbed Hamiltonian, α, incorporates a non-axially-symmetric perturbative term:

$$\alpha_0\to\alpha=\alpha_0+K\,\delta\alpha(\psi,\theta,\zeta), \tag{3}$$

where K is called the stochasticity parameter.

The iterative two-dimensional Tokamap mapping has been constructed from the generating function, δF, of the new momentum, $\psi_{\nu+1}$, and the old angle, θ_ν:

$$\delta F(\psi_{\nu+1},\theta_\nu)=-\frac{1}{(2\pi)^2}\,\frac{\psi_{\nu+1}}{1+\psi_{\nu+1}}\cos 2\pi\theta_\nu. \tag{4}$$

The implicit iterative procedure is

$$\psi_{\nu+1}=\psi_\nu+\frac{K}{2\pi}\,\frac{\psi_{\nu+1}}{1+\psi_{\nu1}}\sin 2\pi\theta_\nu, \tag{5}$$

$$\theta_{\nu+1}=\theta_\nu+W(\psi_{\nu+1})-\frac{K}{(2\pi)^2}\,\frac{1}{(1+\psi_{\nu+1})^2}\cos 2\pi\theta_\nu, \tag{6}$$

where $W(\psi_{\nu+1})$ is the winding number, whose inverse, $q(\psi_{\nu+1})\equiv 1/W$, is the safety factor. Without fluctuations $(K=0)$ this unperturbed q-profile has a radial symmetry and defines the rotation of the magnetic line around a torus. Otherwise when the magnetic field fluctuations exist $(K\neq 0)$ the perturbed q-profile has not the radial symmetry anymore and its 2D dependence in $\{\psi;\theta\}$ space is defined by Eqs. (5) and (6). The simple analytical form of the winding number corresponds to a standard toroidal MHD equilibrium[14] and is realistic for most ohmic discharges:

$$W(\psi)=\frac{w}{4}(2-\psi)(2-2\psi+\psi^2), \tag{7}$$

where w is the value of the winding number on the polar axis.

It has been shown[14,15] that the Tokamap qualitatively reproduces the main features of the magnetic field topology known from tokamak physics: very robust and well-preserved inner field structure near the magnetic axis, chaotic zones and island chains on the main rational magnetic surfaces, Shafranov shift of the magnetic axis, and internal transport barriers to magnetic field line motion near the rational magnetic surfaces.

One of most important map characteristics is a number of fixed points in the phase portrait. The number of the fixed points and their relative position define the type of map phase portrait. The transitions from one type of phase portrait to another can be considered as the bifurcation phenomena. Bifurcation phenomena related to the evolution of the Tokamap fixed points have been analyzed for monotonous[14] and nonmonotonous[16] q-profiles. These phenomena suggest a similarity between the fixed point positions in Tokamap phase portraits and the tokamak magnetic field topology during the crash stage of the sawtooth instability. The Tokamap with monotonous q-profile (7) is characterized by two bifurcation values of the winding number:[14]

$$w_m=1-\frac{K}{(2\pi)^2}, \tag{8}$$

$$w_M=1+\frac{K}{(2\pi)^2}. \tag{9}$$

For the Tokamap with nonmonotonous q-profile there exists an additional bifurcation value, w_b, which cannot be expressed analytically.[16] When the central value of the winding number, w (or the maximal value of the winding number, $w_{\max}$, in the case of a nonmonotonous q-profile), crosses a bifurcation point, the type of the Tokamap phase portrait is changing.

There are three types of Tokamap phase portrait to be used in modeling of the reconnection. (1) In the case of a monotonous q-profile with $w>w_M$ the Tokamap phase portrait has one elliptical fixed point (the center of the crescent magnetic island) and one hyperbolic fixed point (the X-point of reconnection). The polar axis $\psi=0$ is surrounded by robust magnetic surfaces and can be recognized as a magnetic axis. Such a phase portrait is typical of the sawtooth instability in its initial stage. (2) During reconnection the magnetic axis moves toward the X-point, where, in the case of complete reconnection, it disappears (the magnetic axis does not reach the X-point in incomplete reconnection). This stage of reconnection can be modeled by a phase portrait containing two elliptical points (the crescent island and the magnetic axis) and one hyperbolic point (the reconnection X-point). Such a set of fixed points is typical of the Tokamap with nonmonotonous q-profile and with $w_{\max}>w_b$, $w_m<w$

$<w_M$. (3) Finally, the case of complete reconnection, in which the magnetic axis disappears into the reconnection point, is characterized by a phase portrait containing only one elliptical point (corresponding to a monotonous q-profile with $w<w_M$). These three types of the Tokamap phase portrait will be demonstrated during reconnection modeling.

It should be noted that the indicated transitions from one type of Tokamap phase portrait to another can be achieved by evolving the q-profile and K-parameter continuously in time. The transition from the phase portrait with one O-point and one X-point to the phase portrait with two O-points and one X-point occurs when $w=w_M$ (corresponding to the bifurcation of the second O-point on the polar axis). Full reconnection of the magnetic axis corresponds to the transition from case IIB to case IIIB in the presentation of Ref. 16 when $w_{\max}$ reaches w_b. It is clear that the bifurcation values of the winding number depend on K and can therefore be controlled by tuning this parameter.

III. THEORETICAL MODELS OF MAGNETIC RECONNECTION

The existing theoretical models of the sawtooth instability depend critically on the details of the safety factor profile, especially its value on the magnetic axis, q_0. They are based on the stability properties of the internal kink mode with toroidal $n=1$ and poloidal $m=1$ mode numbers. This mode is unstable when q_0 falls below unity.

Two main types of crashes are observed experimentally. While the unstable q-profile with $q_0<1$ is the basic initial condition for all sawtooth experiments, the q_0 value can reach 1 just after crash (full reconnection) or can remain less than 1 (partial reconnection). Kadomtsev proposed the resistive model[8] to explain the mechanism of complete magnetic reconnection. According to this model the internal kink mode grows exponentially during the crash to produce the crescent magnetic island. The crescent island pushes the original magnetic axis away from the plasma center toward the X-point, where the original magnetic axis completely reconnects. At the same time the axis of the magnetic island becomes a new magnetic axis, providing an axial symmetry for the field configuration just after reconnection. The q-profile is equal to unity on the new magnetic axis and is larger than unity elsewhere. The quasi-interchange model of the reconnection[9] describes also the q_0 relaxation to 1 at the crash.

But both Kadomtsev's and the quasi-interchange models of the reconnection do not apply to all experimental observations of the sawtooth instabilities. In particular, they do not describe experiments when q_0 remains below unity after the crash. For this reason alternative models have been proposed, based on the Taylor relaxation process,[11,17] on the magnetic field stochastization[12] and on the incomplete relaxation process.[13] Here the theoretical models of complete and incomplete reconnection will be briefly reviewed according to the presentation given in Ref. 13.

A. Kadomtsev's model of complete reconnection

In the cylindrical approximation, the normalized helical flux of the magnetic field can be expressed as

$$\psi_H(r)=\int_0^r 2r'\left(\frac{1}{q(r')}-1\right)dr', \tag{10}$$

and the normalized toroidal flux is equal to square of the radial coordinate:

$$\psi_T(r)=r^2. \tag{11}$$

Kadomtsev's model of reconnection is based on two assumptions concerning the evolution of the helical and toroidal flux: (1) magnetic surfaces of equal helical flux reconnect and (2) the toroidal flux of the magnetic field is conserved during reconnection. Geometrically, the conservation of toroidal flux corresponds to the conservation of the crescent-shaped area between the reconnected magnetic surfaces.

Due to resistivity, the squeezing of the magnetic surfaces induces a current sheet located around the X-point. This current layer in turn induces changes in the q-profile and dissipates the tokamak magnetic field. The radial maximum of the helical flux corresponds to the radial position of the $q=1$ magnetic surface. During reconnection the value of this maximum does not change, but its radial position moves to the center until the helical flux profile becomes monotonous at the final moment of reconnection. After reconnection the q-profile has low magnetic shear in the central region where the q-values were initially below 1, and satisfies $q(r)\geqslant 1$ everywhere.[18]

B. The incomplete relaxation model

According to the incomplete reconnection model, the reconnection process begins to develop in the same way as in Kadomtsev's model. However, (3) there is a constraining maximum for the crescent island width. When the island width reaches this critical value widespread magnetic turbulence develops in the system. This turbulence stimulates rapid particle and energy transport that collapses plasma confinement. During this process the density and temperature profiles flatten within the reconnection radius.

In contrast to Kadomtsev's model the incomplete reconnection model predicts current sheet formation not only around the X-point but also along the reconnected magnetic surfaces. This condition generates a higher level of magnetic field stochasticity. The central region of the emerging q-profile remains below unity, and regions of low magnetic shear are formed near the plasma core and around the $q=1$ magnetic surface.

Three types of nonlinear behavior have been described for the $m/n=1/1$ resistive mode using a full set of nonlinear resistive magnetohydrodynamic equations.[19] The authors have demonstrated (1) Kadomtsev's reconnection, (2) incomplete reconnection in which the island width initially grows and subsequently shrinks, and (3) saturation, where the island width grows to a limiting value.

IV. MAGNETIC FIELD MAPPING WITH THE TOKAMAP

The Tokamap mapping technique is used to describe the stochastic magnetic field during the crash stage of the sawtooth instability. Theoretical descriptions of reconnection are based primarily on two constraints on the helical and toroidal flux of the magnetic field. These constraints are used to define the evolution of the q-profile and the stochasticity parameter, K, which constitute the complete input data for the mapping. There are no other free parameters in the Tokamap. We will show that both Kadomtsev and incomplete reconnections can be modeled using the Tokamap. As long as maps are considered for describing only the magnetic line topology, they do not contain any information about time. The phase portrait derived from the Tokamap can be seen as a snapshot which is valid for given parameter K and q-profile. If, however, the mapping technique is used to study particle motion, then the particle orbit time around the torus has to be much smaller than the characteristic time for q-profile and K changes.

There are four main stages in the construction of the magnetic field: (1) The evolution of the helical flux is constructed according to the theoretical constraint on the helical flux behavior. (2) The evolving q-profile is derived from the helical flux evolution according to the Eq. (10). (3) The q-profile is introduced to the Tokamap iteration procedure. (4) The value of the stochasticity parameter is chosen to satisfy the theoretical constraint on the toroidal flux. Finally, the topology emerging from the modeled magnetic field is compared with known data.

Theoretical models of the helical flux behavior during the crash stage of the sawtooth instability allow us to establish the corresponding evolution of the q-profile. During the evolution the magnetic surfaces of equal helical flux reconnect and the helical flux has the same value of a maximum at the radius $r_{\max}$, which corresponds to the position of the magnetic surface with $q(r_{\max})=1$.

Throughout the process of both complete and incomplete reconnection there exists a ‘‘mixing radius’’ for the helical flux, which corresponds to the external boundary for the reconnection processes. The helical flux, and consequently the q-profile, does not change outside of this radius during the reconnection.

From a geometrical point of view the toroidal flux of the magnetic field is proportional to the area of the poloidal cross-section. Therefore the evolution of the K value is defined to preserve the area of the crescent magnetic island, which is restricted by the reconnected magnetic surfaces, and consistent with the conservation constraint on the toroidal flux.

A. Simulating Kadomtsev's reconnection

In Kadomtsev's model of reconnection the maximum value of the helical flux does not change during reconnection, while the radial position of the maximum moves toward the center [see Fig. 1(a)]. When the maximum reaches the center the original magnetic axis reconnects completely at the X-point. The evolution of the helical flux inside the radius $r_{\max}$ is constructed in such a way to provide the displacement of the original magnetic axis to the X-point.

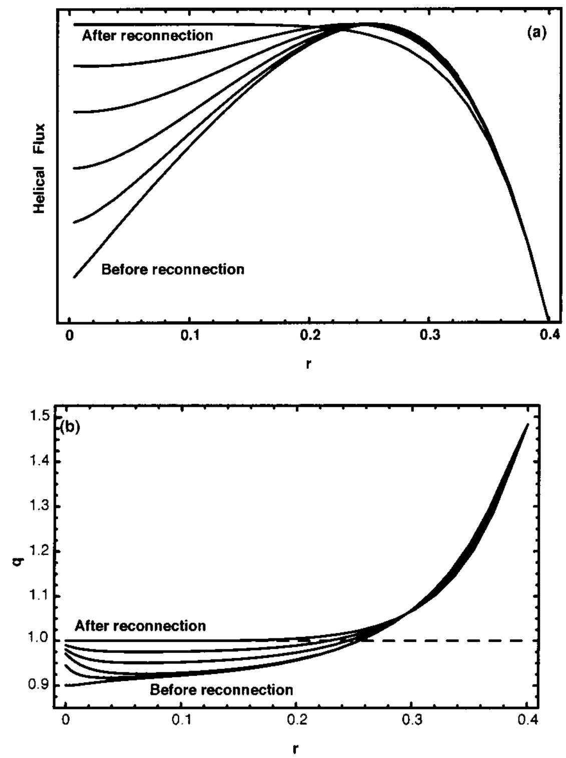

FIG. 1. Evolving dimensionless helical flux (a) and q-profile (b) for the simulation of complete reconnection. Both evolutions have to be considered as a continuous succession from a curve with the minimal value in the center to a curve with the maximal one.

In our model the helical flux function is a one-parameter family of curves, $\psi_{H_\mu}(r)$, where μ is a pseudo-time parameter governing the continuous deformation of the helical flux curve [Fig. 1(a)]. The q-profiles [Fig. 1(b)] are derived from the evolving helical flux function using Eq. (10). In Fig. 1 the evolutions of the helical flux and of the q-profile have to be considered as a succession from a curve with the minimal value in the center to a curve with the maximal one. Figure 1 presents only the central range (in the radial interval [0.0;0.4]) of the normalized helical flux and q-profile dependence, which is changing during reconnection.

The internal kink mode is unstable for q-profiles with $q_0<1$. The behavior of the Tokamap reflects this condition in the following way. When $K=0$, corresponding to an unperturbed magnetic field, the magnetic field structure is robust and axially symmetric and the phase portrait consists of nested circles. But for any nonzero value of K, corresponding even to a small perturbation of the magnetic field, this symmetry is broken. In an asymmetric configuration, the first-order hyperbolic periodic point forms the X-point of reconnection [Fig. 2(a)]. In practice, the magnetic field is perturbed by the current layer that appears at the X-point. Since K reflects the relation between the radial component of magnetic field fluctuations, δB_r, and the characteristic magnetic field amplitude B_0, K is roughly proportional to the generated current in the emergent layer. The initial value of K in the simulation may therefore be related to the magnitude of

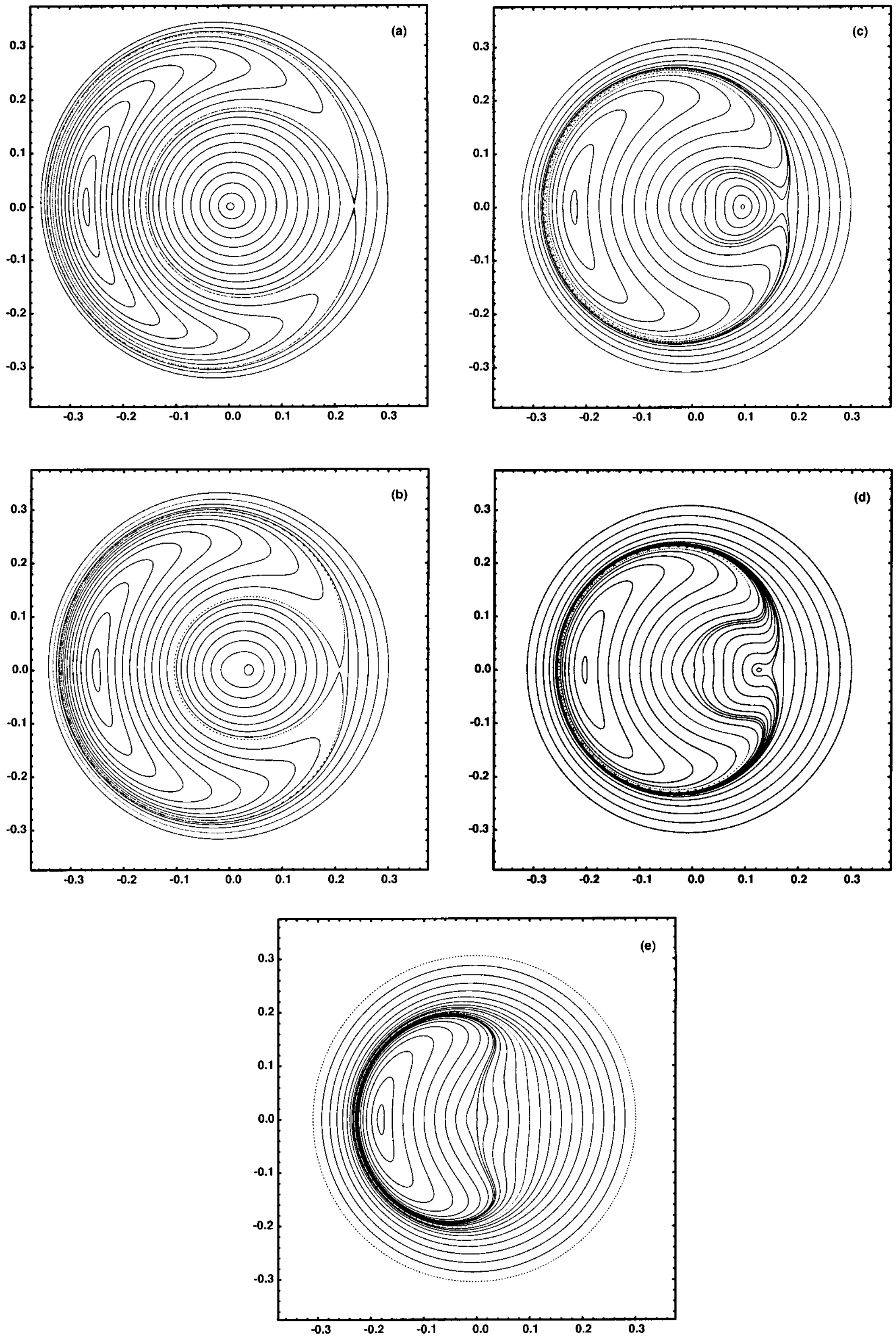

FIG. 2. Tokamap phase portraits illustrating the process of complete reconnection. The values of the stochasticity parameter K are 1.0, 0.65, 0.27, 0.147 and 0.1 in (a)–(e), respectively. The safety factor profile which has been used to build (a) corresponds to the lowest curve of Fig. 1(b). Other used q-profiles are demonstrated in Fig. 3.

the plasma current at the initial stage of reconnection. In the simulations presented here an initial value of $K=1.0$ [Fig. 2(a)] has been chosen to demonstrate the feasibility of this modeling strategy and to illustrate the field topology most clearly. Raising the stochasticity parameter gradually obscures the reconnecting magnetic lines. Nevertheless, other initial values of K correspond to physically similar processes with different levels of magnetic field stochasticity.

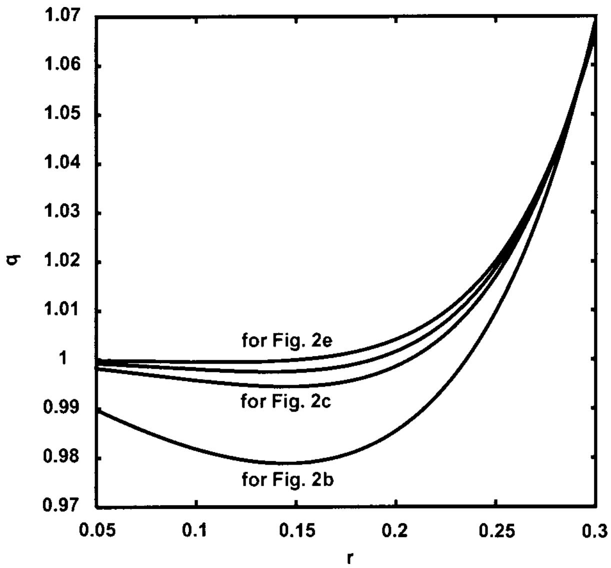

FIG. 3. The safety factor profiles which have been chosen from the succession of Fig. 1(b) to build the phase portraits of the complete reconnection in Figs. 2(b)–2(e).

Figure 2 illustrates the main stages of magnetic reconnection according to Kadomtsev's model. Beginning in Fig. 2(b) ($K=0.65$) the width of the magnetic island gradually increases. The region around the original magnetic axis within the separatrix shrinks due to the outflow of reconnected flux. The original magnetic axis moves from the geometric axis to the X-point as reconnection continues [Fig. 2(c), $K=0.27$]. In Fig. 2(d) ($K=0.147$) the original magnetic axis is already displaced to the edge of the $q=1$ magnetic surface, near the reconnection point. Finally, Fig. 2(e) shows the magnetic field topology just after reconnection with a small level of stochasticity ($K=0.1$), before the magnetic island has completely relaxed to the geometric center. Figures 2(a)–2(e) have been constructed for decreasing values of K from $K=1.0$ in Fig. 2(a) to $K=0.1$ in Fig. 2(e). Such behavior of the K value during reconnection correlates with the gradual disappearance of the current layer, which dissipates the magnetic field at the point of reconnection. The numerically derived safety factor profiles which have been chosen from the succession of Fig. 1(b) to build Figs. 2(b)–2(e) are shown in Fig. 3. Figure 2(a) has been built for the lowest curve of q-profile dependence in Fig. 1(b).

The three types of the Tokamap phase portrait which have been described in Sec. II can be seen now among Fig. 2. Figures 2(a) and 2(e) correspond to the cases with the topology (1) and (3), respectively. Figure 2(c) is the most striking example of second type phase portraits according to the specification of Sec. II.

B. Simulating partial reconnection

The initial evolution of the helical flux is similar in the case of incomplete reconnection, but when the maximum reaches the critical radius (the width of the crescent magnetic island reaches a critical value) its motion to the center is interrupted and the helical flux flattens around the $q=1$ magnetic surface (see Fig. 4a in Ref. 13).

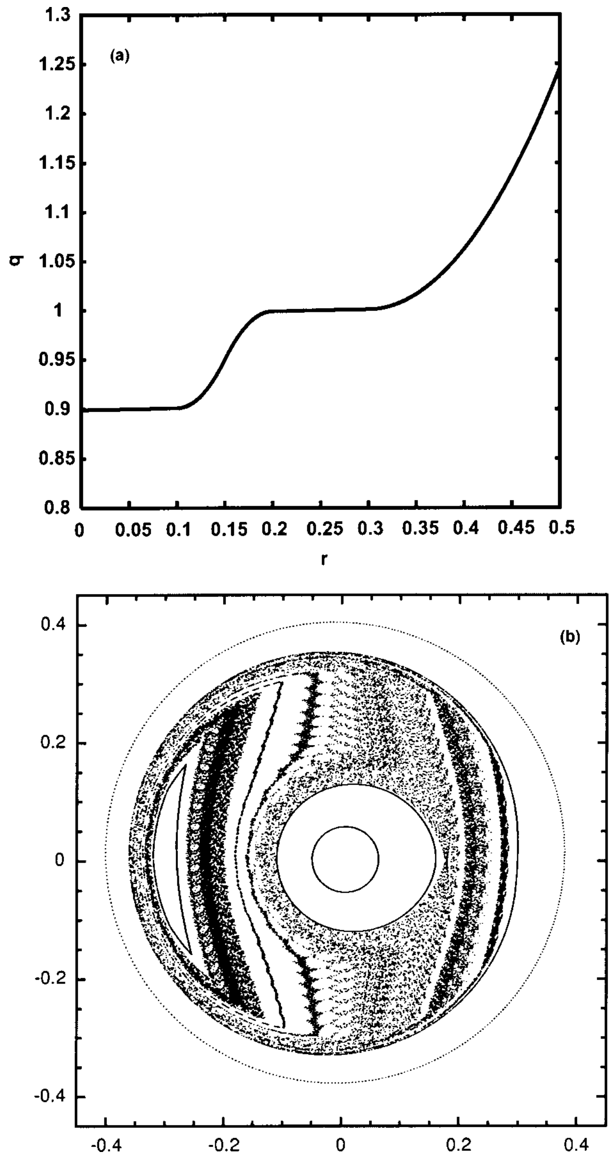

FIG. 4. The safety factor profile (a) and the phase portrait of the incomplete reconnection (b) from the Tokamap simulations. The q-profile is close to the data from Fig. 4 of Ref. 13. The value of the stochasticity parameter has been chosen $K=1.0$.

Incomplete reconnection begins to develop just as Kadomtsev's reconnection does, and for the stages represented in Figs. 2(a)–2(c) the two models give similar predictions. But in the incomplete reconnection model, just as the crescent island reaches a critical width, a current layer spreads out along the reconnected magnetic surfaces, in contrast to Kadomtsev's model, which restricts the current to the region around the X-point. This more complicated current structure gives rise to an increased magnetic field stochasticity and enhances the turbulent transport causing the collapse of plasma confinement.

Figure 4 demonstrates the magnetic field topology at the final stage of the incomplete reconnection with the q-profile dependence close to the data from Fig. 4 in Ref. 13. As an example, the q-profile has been chosen with the low shear regions in the central range [0;0.1] with $q_0 \approx 0.9$ and in the radial interval [0.2;0.3] with the $q(r) \approx 1.0$. The q-profile

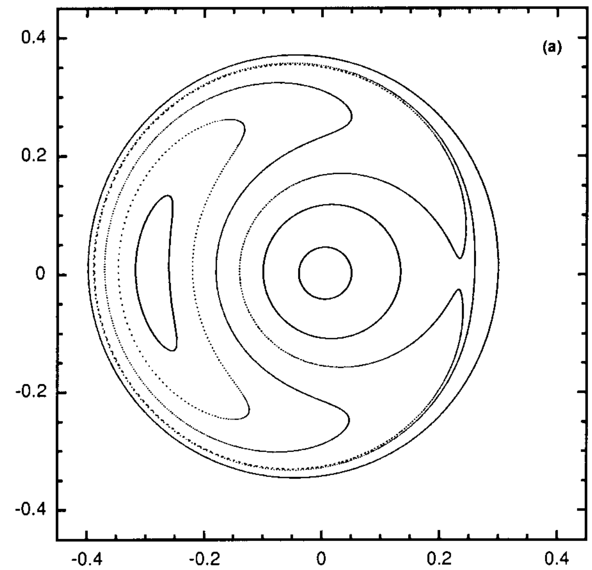

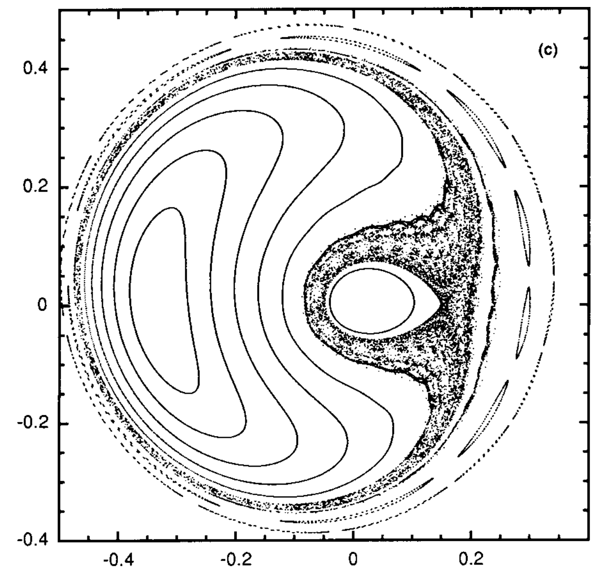

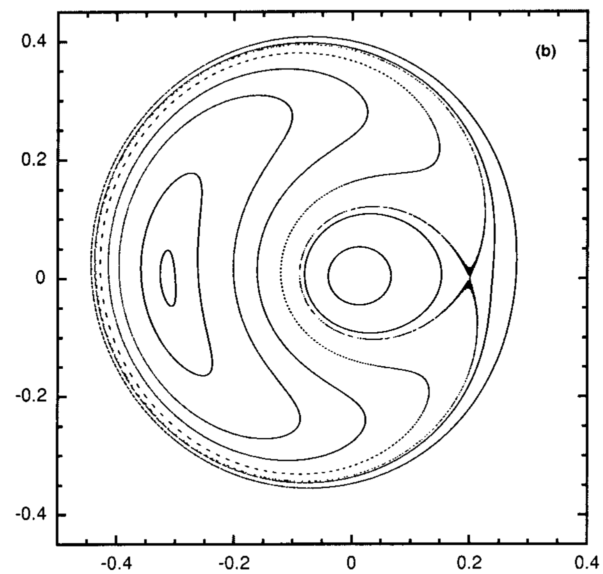

FIG. 5. The phase portraits of the partial reconnection with the different values of the magnetic field stochasticity from the Tokamap simulations. The figures have been built for the standard q-profile from Eq. (7) with $q_0 = 0.9$ and $K = 1.0$, $K = 2.0$, $K = 3.0$ in (a)–(c), respectively.

between two flat regions is changing smoothly. In the simulation $K = 1.0$. The topology of the magnetic field in Fig. 4(b) demonstrates the widespread magnetic turbulence everywhere between the reconnected magnetic surfaces in accordance with the incomplete reconnection description in Ref. 13.

The stochastic model[12] predicts the partial reconnection even with the monotonous q-profile. In this model the magnetic field stochasticity develops around, but not necessarily everywhere between, the reconnected surfaces. Figure 5 demonstrates the magnetic field topology in the case of the partial reconnection with the different levels of the magnetic field stochasticity. They have been built for the standard q-profile from Eq. (7) with $q_0 = 0.9$ and different values of the stochasticity parameters K [$K = 1.0$ in Fig. 5(a), $K = 2.0$ in Fig. 5(b) and $K = 3.0$ in Fig. 5(c)]. For small values of the stochasticity parameter [Fig. 5(a)] the X-point can be seen without a visible formation of the stochastic layer. With increasing the stochasticity parameter value the stochastic domain around the X-point becomes more and more remarkable [Fig. 5(b)] and the stochastic layer is formed and grows around the reconnected surfaces [Fig. 5(c)].

In the case of the partial reconnection with the monotonous q-profile the larger magnetic field stochasticity provides smaller q_0 value for the same saturated island. For example, according to Eq. (9) the standard q-profile dependence (7) with the stochasticity value $K = 3.0$ describes the X-point of the reconnection in the Tokamap phase portrait if $q_0 < 0.925$. In this way the model of the partial reconnection with the final stochasticity $K = 3.0$ cannot provide q_0 larger than 0.925 if we will try to use the safety factor profile closed to the standard one. Such limit values of q_0 can be calculated for any chosen q-profile dependence from the analysis of the Tokamap fixed point taking into consideration the bifurcation phenomena of the phase portrait. These studies confirm the important role of the magnetic stochasticity in the case of the partial magnetic reconnection[12] and the qualitative relation between the level of the magnetic stochasticity and q_0 value after reconnection.

In this way the introduction of the complete reconnection model by Ref. 13 in the Tokamap allows us to reproduce (Fig. 2) the magnetic field topology of the complete reconnection known from the literature (Fig. 11 of Ref. 19 and Fig. 7 of Ref. 20). Flattened q-profile dependence around $q=1$ demonstrates the increased magnetic field stochasticity between the reconnected magnetic surfaces (Fig. 4) in accordance with the incomplete reconnection modeled by Ref. 13. The important role of the magnetic field stochasticity in the case of the partial reconnection is shown in Fig. 5, which closely resembles Fig. 16 of Ref. 19 and Fig. 4 of Ref. 12.

V. DEPENDENCE OF THE RECONNECTION PHASE PORTRAIT ON THE SAFETY FACTOR PROFILE

In the previous section the description of the crash stage of magnetic reconnection has been demonstrated starting from the monotonous q-profile with a minimum value $q_0=0.9$ and for the particular value of the conserved toroidal flux which is proportional to the area of the magnetic island in Fig. 2. The island area has been specified by the initial value of the stochasticity parameter (here $K=1.0$). Really the crash modeling can start from any q-profile with the region $q(r)<1$ and the value of the stochasticity parameter K will define the value of the toroidal flux which is conserved. For example, it has been shown in Ref. 14 for the standard q-profile (7) with $q_0=0.9$ that there exists an X-point in the Tokamap phase portrait for $0<K<4\pi^2(1/q_0-1)\approx 4.3865$. It means any K value from this range will define a unique area of the magnetic island.

For the arbitrary q-profile with a radial region $q(r)<1$, the limiting value of the stochasticity parameter, K_{lim}, which defines the stochasticity range $0<K<K_{lim}$ for which the Tokamap phase portrait contains a hyperbolic fixed point, can be calculated numerically. It is significant that the position of the X-point (the area of the magnetic island) depends on both the q-profile and the K value. This implies the Tokamap can describe the reconnection process of magnetic field for different initial q-profiles and for different initial values of magnetic field stochasticity but the evolution of these specifications is constructed from the theoretical constrains.

Furthermore, the evolution of the stochasticity parameter value determines whether the reconnection process is complete ($q\geqslant 1$ everywhere after crash) or incomplete ($q<1$ somewhere after crash). The process of complete reconnection can be described only by requiring that the level of stochasticity will be low at the final stage of reconnection. In the simulation presented here we left $K=0.1$ after reconnection in the complete reconnection model. In the same time the lower levels of magnetic fields stochasticity provide larger values of q_{min} at the final stages of the incomplete reconnection.

In accordance with theoretical constraints and the bifurcation properties of the Tokamap, the complete reconnection can be described correctly only by using q-profiles having negative magnetic shear in the central region [that is, for $q(r)$ satisfying $d\log(q)/d\log(r)<0$ somewhere inside r_{max}]. But it should be noted here that the input winding number, $W(\psi)$, of the Tokamap iteration procedure (5) is close to the perturbed winding number only for small values of the stochasticity parameter. So it is important to realize that the experimentally measured q-profile is closer to the perturbed q-profile in the mapping description. Therefore, in general, in the case of the complete reconnection the description of the magnetic reconnection is not restricted by the negative value of the perturbed magnetic shear inside the radius r_{max} but the input magnetic shear of the Tokamap should become negative inside this radius during the crash.

It will be shown in a forthcoming work that even small local changes in the q-profile or its derivatives have essential effect on the magnetic field topology. An additional direction for further study would be to seek an explicit relationship between the stochasticity parameter, K, and the magnitude of magnetic field fluctuations. Such a relationship could enable the Tokamap to be used in reconstructing q-profiles from experimental data.

VI. CONCLUSIONS

It has been shown that the mapping technique Tokamap, which has been proposed for the description of the magnetic field topology in tokamaks, is also a good tool to obtain the poloidal cross section of the magnetic field topology during the crash stage of the sawtooth instability. To this end, it was necessary to link the mapping technique to the theoretical models of the sawtooth instability and to compare the resulting phase portraits with experimental evidences.

The radial dependence of the helical flux (derived q-profile dependence) and the stochasticity parameter K at the moment when the instability is triggered are free specifications of the simulation. It does not conflict with the theoretical models of the sawtooth instability where the instability can be triggered for any q-profile if there is a region with $q(r)<1$. Also the radial fluctuations of the magnetic field at the initial stage of the crash depend on the value of the current generated around the X-point and will define the value of the stochasticity parameter K at this moment. Therefore, although the initial q-profile dependence and the initial stochasticity parameter K are the free specifications of the model, they can be obtained or, at least, estimated from the experimental data at the moment when the instability is triggered. But if there is such justification of the q-profile dependence and K data at the initial stage of the crash there are clear rules (see Sec. III A) to map the magnetic field topology during the crash stage of the complete reconnection.

The simulation of the incomplete reconnection has another free parameter. It is a saturated width of the crescent magnetic island. Then some scenarios of the incomplete reconnection can start to develop from the different q-profile dependence and K data and reach the same saturated island width at the final stage of the crash.

Following the procedure described in Sec. IV, we have determined the evolution of the q profile and of the stochasticity parameter that are compatible with the theories of the sawtooth instability and with the experiments for both the complete and the incomplete magnetic reconnection cases.

ACKNOWLEDGMENTS

This work has been carried out within the Association EURATOM-Etat Belge. The content of the publication is the sole responsibility of its publishers and it does not necessarily represent the views of the Commission or its services. We would like to thank Professor R. Balescu, Dr. J. H. Misguich, Dr. D. Constantinescu and Dr. G. Steinbrecher for many fruitful discussions.

[1] J. O'Rourke, Plasma Phys. Controlled Fusion **33**, 289 (1991).
[2] M. Yamada, F. M. Levinton, N. Pomphrey, R. Budny, J. Manickam, and Y. Nagayama, Phys. Plasmas **1**, 3269 (1994).
[3] F. M. Levinton, S. H. Batha, M. Yamada, and M. C. Zarnstorff, Phys. Fluids B **5**, 2554 (1993).
[4] D. Wróblewski and L. L. Lao, Phys. Fluids B **3**, 2877 (1991).
[5] G. J. Kramer, C. Z. Cheng, Y. Kusama, R. Nazikian, S. Takeji, and K. Tobita, Nucl. Fusion **41**, 1135 (2001).
[6] G. J. Kramer, T. Oikawa, T. Fujita, Y. Kamada, Y. Kusama, K. Tobita, T. Ozeki, C. Z. Cheng, and R. Nazikian, Plasma Phys. Controlled Fusion **40**, 863 (1998).
[7] H. A. Holties, A. Fasoli, J. P. Goedbloed, G. T. A. Huysmans, and W. Kerner, Phys. Plasmas **4**, 709 (1997).
[8] B. B. Kadomtsev, Sov. J. Plasma Phys. **1**, 389 (1975).
[9] J. A. Wesson, Plasma Phys. Controlled Fusion **28**, 243 (1986).
[10] Ya. I. Kolesnichenko, Yu. V. Yakovenko, D. Anderson, M. Lisak, and F. Wising, Phys. Rev. Lett. **68**, 3881 (1992).
[11] C. G. Gimblett and R. J. Hastie, Plasma Phys. Controlled Fusion **36**, 1439 (1994).
[12] A. J. Lichtenberg, K. Itoh, S.-I. Itoh, and A. Fukuyama, Nucl. Fusion **32**, 495 (1992).
[13] F. Porcelli, D. Boucher, and M. N. Rosenbluth, Plasma Phys. Controlled Fusion **38**, 2163 (1996).
[14] R. Balescu, M. Vlad, and F. Spineanu, Phys. Rev. E **58**, 951 (1998).
[15] J. H. Misguich, Phys. Plasmas **8**, 2132 (2001).
[16] R. Balescu, Phys. Rev. E **58**, 3781 (1998).
[17] J. B. Taylor, Rev. Mod. Phys. **58**, 741 (1986).
[18] W. J. Goedheer and E. Westerhof, Nucl. Fusion **28**, 565 (1988).
[19] L. A. Charlton, B. A. Carreras, J. A. Holmes, and V. E. Lynch, Phys. Fluids **31**, 347 (1988).
[20] W. Park, D. A. Monticello, and R. B. White, Phys. Fluids **27**, 137 (1984).